Fluorescence Studies on the Nucleotide Binding Domains of the P-Glycoprotein Multidrug Transporter†

Ronghua Liu and Frances J. Sharom*

Guelph-Waterloo Centre for Graduate Work in Chemistry, Department of Chemistry and Biochemistry, University of Guelph, Guelph, Ontario, Canada N1G 2W1

Received October 29, 1996; Revised Manuscript Received January 8, 1997⊗

ABSTRACT: One of the major causes of multidrug resistance in human cancers is expression of the P-glycoprotein multidrug transporter, which acts as an efflux pump for a diverse range of natural products, chemotherapeutic drugs, and hydrophobic peptides. In the present study, fluorescence techniques were used to probe the nucleotide binding domains (NBD) of P-glycoprotein. The transporter was labeled at two conserved cysteine residues, one within each NBD, using the thiol-reactive fluor 2-(4′-maleimidyl-anilino)-naphthalene-6-sulfonic acid (MIANS), and collisional quenching was used to assess solvent accessibility of the bound probe. Acrylamide was a poor quencher, which suggests that MIANS is buried in a relatively inaccessible region of the protein. Iodide ion was a highly effective quencher, whereas Cs^+ was not, demonstrating the presence of a positive charge in the region close to the ATP binding site. The fluorescent nucleotide derivative 2′(3′)-*O*-(2,4,6-trinitrophenyl)-ATP (TNP-ATP) was hydrolysed slowly by P-glycoprotein, with a V_{max} ∼20-fold lower than that for unmodified ATP, and a K_M of 81 μM. TNP-ATP and TNP-ADP inhibited P-glycoprotein ATPase activity, indicating that they interact with the NBD, whereas TNP-AMP was a very poor inhibitor. When TNP-nucleotides bound to P-glycoprotein, their fluorescence intensity was enhanced in a concentration-dependent manner. Both TNP-ATP and TNP-ADP bound to P-glycoprotein with substantially higher affinity than ATP, with K_d values of 43 and 36 μM, respectively. Addition of ATP led to only partial displacement of TNP-ATP. Resonance energy transfer was observed between cysteine-bound MIANS and TNP-ATP/ADP, which indicated that the two fluorescent groups are located close to each other within the catalytic site of P-glycoprotein.

P-Glycoprotein (Pgp)[1] is a member of the ABC (ATP-binding cassette) superfamily of membrane transporters (Higgins, 1992; Doige & Ames, 1993). Overexpression of this 170 kDa plasma membrane glycoprotein results in multidrug resistance, both in cultured cell lines *in vitro* and human tumours *in vivo* (Gottesman & Pastan, 1993; Leveille-Webster & Arias, 1995; Lehnert, 1996). Its sequence similarity to other eukaryotic and prokaryotic transporters led to the proposal that Pgp is an ATP-driven drug efflux pump for a diverse range of natural products. Pgp is expressed in several normal tissues, including the apical surfaces of the cells of the intestine, the bile canalicular membranes, and the endothelial cells of capillaries of the blood brain barrier. Its physiological role has been assumed to involve protection of tissues from toxic xenobiotics by efflux/excretion. This postulate has been substantiated by the recent generation of transgenic mice with a genetic disruption of the *mdr1a* gene encoding Pgp. Lack of functional Pgp resulted in altered tissue distribution and pharmacokinetics, as well as greatly increased toxicity, for drugs such as vinblastine, cyclosporin A, and ivermectin (all known Pgp substrates) (Schinkel et al., 1995). Many normally non-toxic drugs were also able to penetrate the brain in *mdr1a* (−/−) mice (Schinkel et al., 1996).

Reconstitution studies have recently shown that Pgp functions as an active ATP-driven transporter for chemotherapeutic drugs (Sharom et al., 1993; Sharom, 1995; Shapiro & Ling, 1995) and hydrophobic peptides (Eytan et al., 1994; Sharom et al., 1995a, 1996). However, very little is currently known about the details of the transport cycle or the mechanism by which ATP hydrolysis energizes drug transport. Detailed studies using active purified Pgp are required to make any progress in this area.

Pgp is predicted to be composed of two homologous halves, each comprising six hydrophobic membrane spanning segments and a consensus sequence for a nucleotide binding domain (NBD). The NBDs of Pgp contain the Walker A and B motifs characteristic of the ABC superfamily (Walker et al., 1982) and are located on the cytoplasmic side of the membrane. Highly purified Pgp displays constitutive AT-Pase activity, which is atypical for an ATP-driven transporter, and the K_M for hydrolysis of nucleotides is also unusually high, in the range 0.4−0.8 mM (Doige et al., 1992; Urbatsch et al., 1994; Shapiro & Ling, 1994; Sharom et al., 1995b). The ATPase activity of Pgp is modulated, both positively and negatively, by binding of substrates to the drug binding site of the transporter (Doige et al., 1992; Urbatsch et al., 1994; Shapiro & Ling, 1994; Sharom et al., 1995a, 1995b),

† This work was supported by a grant to FJS from the National Cancer Institute of Canada, with funds provided by the Canadian Cancer Society.

* To whom correspondence should be addressed (telephone, 519-824-4120, ext 2247; Fax, 519-766-1499; e-mail, sharom@chembio.uoguelph.ca).

⊗ Abstract published in *Advance ACS Abstracts,* February 15, 1997.

[1] Abbreviations: CHAPS, 3-[(3-cholamidopropyl)-dimethylammonio]-1-propanesulfonate; DTE, dithioerythritol; MDR, multidrug resistance; MIANS, 2-(4′-maleimidylanilino)naphthalene-6-sulfonic acid; NBD, nucleotide binding domain; Pgp, P-glycoprotein; TNP-ADP, 2′-(3′)-*O*-(2,4,6-trinitrophenyl)adenosine 5′-diphosphate; TNP-AMP, 2′-(3′)-*O*-(2,4,6-trinitrophenyl)-adenosine 5′-monophosphate; TNP-ATP, 2′(3′)-*O*-(2,4,6-trinitrophenyl)adenosine 5′-triphosphate.

S0006-2960(96)02711-0 CCC: $14.00

which is believed to be located within the membrane-spanning regions of the protein. This modulation indicates the existence of communication, or coupling, between the drug binding site(s) and the catalytic site for ATP hydrolysis within the NBD. We recently used fluorescence spectroscopy to observe this coupling directly, and demonstrated that binding of drugs leads to a conformational change in the NBD (Liu & Sharom, 1996). This conformational change is presumed to play a central role in the coupling of drug transport to ATP hydrolysis.

In the absence of any information on the 3-dimensional structure of the multidrug transporter, powerful spectroscopic techniques such as fluorescence can provide valuable details about both the molecular architecture of the Pgp molecule, and the dynamics of its interactions with ATP and drugs. The present report is the first to use fluorescence techniques to examine the molecular characteristics of the NBDs of purified full-length Pgp with very high specific ATPase activity. We have employed two complementary applications of fluorescence spectroscopy. First, collisional quenching was used to investigate the charge and hydrophobicity of the catalytic site region of the NBD. To accomplish this, the fluorescent probe (MIANS) was placed on two highly conserved cysteine residues, one within each NBD of Pgp (Liu & Sharom, 1996). In the second approach, we examined the effects of fluorescent 2′(3′)-*O*-(2,4,6-trinitrophenyl) (TNP) nucleotide derivatives on the ATPase function of Pgp and characterized the interaction of these molecules with the NBD.

MATERIALS AND METHODS

Materials. Asolectin was obtained from Fluka (Ronkonkoma, NY). 3-[(3-Cholamidopropyl)-dimethylammonio]-1-propanesulfonate (CHAPS), dithioerythritol (DTE), and disodium-ATP were purchased from Sigma Chemical Co. (St. Louis, MO). MIANS, TNP-ATP, TNP-ADP, and TNP-AMP were supplied by Molecular Probes (Eugene, OR).

MDR Cell Lines and Pgp Purification. Plasma membrane vesicles from the MDR chinese hamster ovary cell line CH^R-B30 (Ling & Thompson, 1974) were isolated as described previously (Doige & Sharom, 1991; Liu & Sharom, 1996). Pgp was purified to 95% purity by a procedure involving a differential two-step extraction of CH^RB30 plasma membrane with CHAPS, followed by removal of contaminant glycoproteins on concanavalin A-Sepharose (Liu & Sharom, 1996). The final Pgp preparation (50−100 μg/mL in buffer consisting of 2 mM CHAPS/50 mM Tris-HCl/0.15 M NH_4Cl/5 mM $MgCl_2$/0.02% NaN_3, pH 7.5) was kept on ice and used within 24 h. Protein was quantitated by the method of Bradford (1976) for plasma membrane and by the method of Peterson (1983) for purified Pgp, using bovine serum albumin (crystallized and lyophilized, Sigma) as a standard.

Measurement of Pgp ATPase Activity. Mg^{2+}-ATPase activity of Pgp was determined by measuring the release of inorganic phosphate from ATP or TNP-ATP, in the presence of 5 mM Mg^{2+}, as described previously (Doige et al., 1992; Sharom et al., 1995a). The assay was extended to 90 min for TNP-ATP because of the slow rate of hydrolysis. To quantitate inhibition of Pgp ATPase, various concentrations of fluorescent nucleotides were included in the ATPase assay, followed by incubation at 37 °C.

MIANS Labeling of Pgp. Pgp was specifically labeled with MIANS at the two cysteine residues in the NBDs as described (Liu & Sharom, 1996). Purified Pgp (100 μg/mL in 2 mM CHAPS buffer) was incubated with 20 μM MIANS at 22 °C for 1 h in the dark. Unreacted MIANS was quenched with 1 mM DTE, and the MIANS-labeled Pgp was separated by gel filtration on Bio-Gel P-6 (Bio-Rad Laboratories, Mississauga, ON) equilibrated with 2 mM CHAPS buffer. The final concentration of MIANS-labeled Pgp was ∼50 μg/mL. As a control, MIANS was reacted with the soluble sulfhydryl-containing molecule, DTE.

Fluorescence Measurements. Fluorescence was measured at 22 °C using a Spex Model DM3000 spectrofluorimeter (Spex Industries Inc., Edison, NJ), with excitation and emission slits set to 4 nm. For MIANS-labeled Pgp, excitation was carried out at 322 nm, and fluorescence emission was recorded at 420 nm (Liu & Sharom, 1996). Fluorescence emission spectra and steady-state fluorescence emission intensities for TNP-ATP and TNP-ADP were recorded using an excitation wavelength of 408 nm. All fluorescent studies using purified Pgp (except collisional quenching experiments) were performed in the presence of 0.5 mg/ml asolectin (soybean phospholipids), which was added as extruded 100 nm unilamellar vesicles (MacDonald et al. 1991; Liu & Sharom, 1996).

Collisional Quenching Studies using MIANS-Pgp. Stock solutions of 5 M acrylamide (Bio-Rad Laboratories, Mississauga, ON), 5 M KI (Fisher Scientific, Unionville, ON), and 5 M CsCl (Fisher Scientific) were added as 5 μL aliquots in 2 mM CHAPS buffer to 0.5 mL of 50 μg/mL MIANS-Pgp in the same buffer. All quencher solutions were prepared fresh, and 0.1 mM $Na_2S_2O_3$ was added to the KI stock solution to prevent I_3-formation. Fluorescence intensities were corrected for dilution and scattering, and in control assays, KCl was added at the same concentrations to correct for any ionic strength effects. Parallel experiments were carried out using MIANS-DTE, to assess quenching of MIANS by the same agents when completely accessible in aqueous solution. Acrylamide, I^-, and Cs^+ quenching data were analyzed using the Stern−Volmer equation (Lakowicz, 1983),

$$F_0/F = 1 + k_q\tau_o[Q] = 1 + K_{sv}[Q]$$

where F_0 and F are the fluorescence intensities in the absence and presence of quencher, respectively, k_q is the bimolecular quenching constant, τ_o is the fluorescence lifetime in the absence of quencher, [Q] is the concentration of quenching agent, and K_{sv} is the Stern−Volmer quenching constant. A Stern−Volmer plot of F_0/F vs [Q] gives a linear plot with a slope of K_{sv}.

Fluorescence Enhancement Studies Using TNP-Nucleotide Derivatives. The affinity of TNP-ATP and TNP-ADP for binding to Pgp was determined by titrating a fixed amount of purified Pgp (500 μL of 50 μg/mL Pgp in 2 mM CHAPS buffer in a 0.5 cm quartz cuvette) at 22 °C with increasing concentrations of fluorescent nucleotide. After each addition, the steady-state fluorescence was measured at the emission maximum for each fluor, using excitation at 408 nm. Data were corrected for dilution, scattering, and the inner filter effect as described previously (Liu & Sharom, 1996). Control titrations were performed in the absence of Pgp, and the fluorescence intensities were subtracted from those recorded in the presence of Pgp. The fluorescence enhancement observed in the presence of Pgp was assumed to be

proportional to the concentration of Pgp-bound nucleotide and was plotted as a function of the total fluorescent nucleotide concentration added.

Data from fluorescence enhancement studies were computer-fitted to the following equation, describing interaction with a single type of binding site,

$$\Delta F = \frac{\Delta F_{max} \times [S]}{K_d + [S]}$$

where ΔF represents the change in fluorescence intensity following addition of nucleotide at a concentration [S], ΔF_{max} is the maximum change in fluorescence intensity, and K_d is the dissociation constant. Fitting was performed using nonlinear regression with the Marquardt−Levenberg algorithm (SigmaPlot for Windows, Jandel Scientific), and values of K_d were extracted.

Fluorescence Quenching of MIANS-Pgp by TNP-Nucleotide Derivatives. The fluorescence emission spectrum of MIANS-labeled Pgp (50 μg/mL in 2 mM CHAPS buffer with 0.5 mg/mL phospholipids) was recorded following excitation at 322 nm, in either the absence or presence of 30 μM TNP-ATP. To quantitate the quenching of MIANS by TNP nucleotides, MIANS-labeled Pgp was titrated at 22 °C with increasing concentrations of TNP-ATP or TNP-ADP.

RESULTS

Pgp Isolation and MIANS Labeling. We previously described the isolation of Pgp from MDR CH^RC5 and CH^R-B30 chinese hamster ovary cells, using a selective two-step extraction with the detergent CHAPS followed by removal of glycoprotein contaminants by concanavalin A-Sepharose chromatography (Sharom et al., 1995b; Liu & Sharom, 1996). The Pgp used in this study was ~95% pure (Liu & Sharom, 1996) and displayed very high basal ATPase specific activity, with a V_{max} of around 3 μmol min^{-1} (mg of protein)$^{-1}$. Site-specific fluorescence labeling of purified Pgp at Cys 428 and Cys 1071 within the Walker A motifs of the NBD was achieved using the thiol-specific probe, MIANS. MIANS labeling inactivates the ATPase function of Pgp, but ATP can still bind to the active site with similar affinity (Liu & Sharom, 1996). Fluorescence studies on MIANS-labeled and native Pgp were carried out in the presence of phospholipids, which assist in the attainment of a more native conformation.

Solvent Accessibility of MIANS Bound to the NBD of Pgp. Fluorescence quenching has proved to be a very useful technique not only to study the aqueous accessibility of fluorescent groups bound to proteins, but also to provide information on the polarity and charge of the region in the vicinity of the bound probe. Three collisional quenchers, acrylamide, I^-, and Cs^+, were used to assess the solvent accessibility and local environment of MIANS bound to the NBD of Pgp. In each case, a parallel experiment was performed with MIANS bound to the small soluble molecule DTE. As shown in Figure 1, Stern−Volmer plots for quenching of MIANS-Pgp were linear for each of the three quenchers; the absence of multiple components indicates that a single class of quenched fluors exists within the protein. The two bound MIANS molecules, one within NBD1, the other within NBD2, therefore appear to behave virtually identically to each other. The Stern−Volmer quenching constant, K_{sv}, was determined in each case (Table 1).

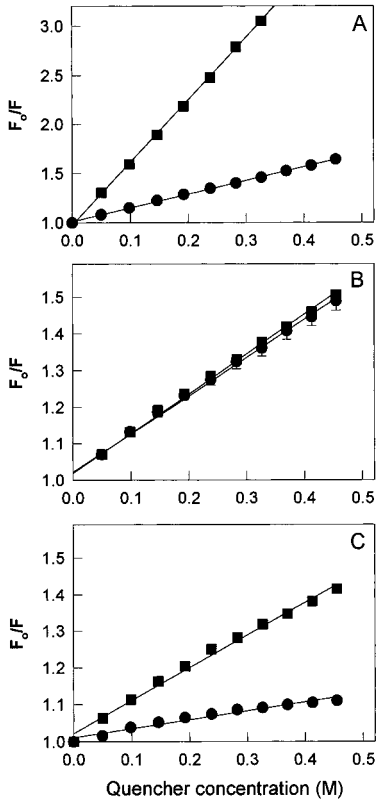

FIGURE 1: Stern−Volmer plots for quenching of MIANS-Pgp and MIANS-DTE by (A) acrylamide, (B) iodide ion I^-, and (C) cesium ion Cs^+. Aliquots (5 μL) of 5 M solutions of acrylamide, KI, and CsCl were added at 22 °C to 0.5 mL of 50 μg/mL MIANS-Pgp in 2 mM CHAPS buffer. Parallel experiments were carried out using MIANS-Pgp (●) and MIANS-DTE (■). Fluorescence intensities were corrected for dilution, scattering, and ionic strength effects.

Table 1: Stern−Volmer Constants for Collisional Quenching of MIANS-Pgp and MIANS-DTE

	K_{sv} (M^{-1})[a]		
	acrylamide	I^-	Cs^+
MIANS-Pgp	1.42 ± 0.01	1.11 ± 0.02	0.27 ± 0.01
MIANS-Pgp + 2 mM ATP	1.29 ± 0.01	0.75 ± 0.01	0.42 ± 0.01
MIANS-DTE	6.29 ± 0.02	1.14 ± 0.02	0.97 ± 0.02

[a] K_{sv} values were determined from the slopes of Stern−Volmer plots of the type shown in Figure 1, for both MIANS bound to Pgp, and MIANS bound to the small soluble molecule DTE. Two independent experiments were carried out, and K_{sv} values were generated by computer-fitting (mean ±95% confidence interval).

MIANS bound to Pgp was quenched poorly by acrylamide, compared to the quenching observed for the fluor bound to DTE, where it is completely accessible in aqueous solution (Figure 1A). This finding shows that the probe is protected from the external environment when bound to the cysteine residues within the NBD, likely because it is buried within the protein structure. Cs^+ was also a poor quencher of MIANS fluorescence (Figure 1C), whereas I^- was a highly effective quencher of MIANS-Pgp, which was quenched similarly to MIANS-DTE (Figure 1B). The results obtained with the charged quenchers suggest that the region around the MIANS-labeled cysteine is positively charged, so that cesium ion cannot approach the probe, whereas the negatively charged I^- ion is attracted into that area of the protein and thus quenches very efficiently.

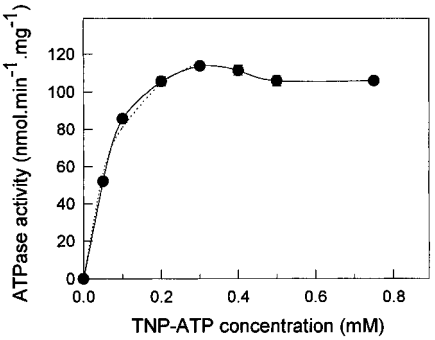

FIGURE 2: Kinetics of TNP-ATP hydrolysis by purified Pgp. Hydrolysis of TNP-ATP was measured at different concentrations of the nucleotide derivative, and the data up to 0.3 mM TNP-ATP were fitted to the Michaelis−Menten equation using nonlinear regression analysis. The calculated best-fit curve for a K_M of 81 μM and V_{max} of 0.147 μmol min^{-1} (mg of protein)$^{-1}$ is indicated by the dotted line. V_{max} for hydrolysis of unmodified ATP by the same Pgp preparation was 2.81 μmol min^{-1} (mg of protein)$^{-1}$.

Quenching experiments carried out in the presence of ligand can also indicate the existence of conformational changes arising from ligand binding. Accordingly, we repeated the quenching experiments using acrylamide in the presence of 2 mM ATP, which is sufficient for complete occupancy of the NBD (Liu & Sharom, 1996). The slope of the Stern−Volmer plot decreased by ~10% compared to that determined in the absence of ATP (Table 1). Therefore, it appears that the conformational change induced in the NBD by ATP binding makes the bound MIANS within the catalytic site less accessible to acrylamide. When the NBD is occupied by ATP, I^- is substantially less effective as a quencher, as indicated by a decrease in the value of K_{sv} (Table 1). ATP likely partially shields the positive charge in the active site region, decreasing the attraction of I^- to this region, and may also sterically block the quencher from gaining access to the MIANS group. Conversely, the K_{sv} for quenching by Cs^+ is increased when the NBD is occupied by ATP (Table 1), as expected if ATP partially screens the positive charge.

TNP-Nucleotide Derivatives as Substrates and Inhibitors of Pgp ATPase. The fluorescent nucleotide derivatives TNP-ATP, TNP-ADP, and TNP-AMP have proved useful in the characterization of nucleotide-binding sites in enzymes and transporters. TNP-ATP was hydrolyzed slowly by Pgp (Figure 2), with a V_{max} of 147 ± 8 nmol min^{-1} (mg of protein)$^{-1}$, compared to 2.81 ± 0.13 μmol min^{-1} (mg of protein)$^{-1}$ for hydrolysis of unmodified ATP by the same Pgp preparation. ATP bearing the bulky TNP group, therefore, is hydrolyzed 19-fold slower than unmodified ATP. The K_M for TNP-ATP hydrolysis was 81 ± 10 μM, substantially lower than the K_M for ATP, which is around 0.5 mM (Sharom et al., 1995b).

The ability of the three TNP nucleotide derivatives to inhibit Pgp ATPase activity was determined by kinetic measurements at different concentrations of the nucleotides (Figure 3A,B,C). Both TNP-ATP and TNP-ADP were good inhibitors of Pgp ATPase activity (Figure 3A,B), whereas TNP-AMP was a poor inhibitor, even at relatively high concentrations (Figure 3C). TNP-ATP was a classical competitive inhibitor, as shown by Lineweaver−Burk analysis (Figure 3D), with a K_i of 111 ± 7 μM. TNP-ADP inhibited ATPase activity more effectively than the same

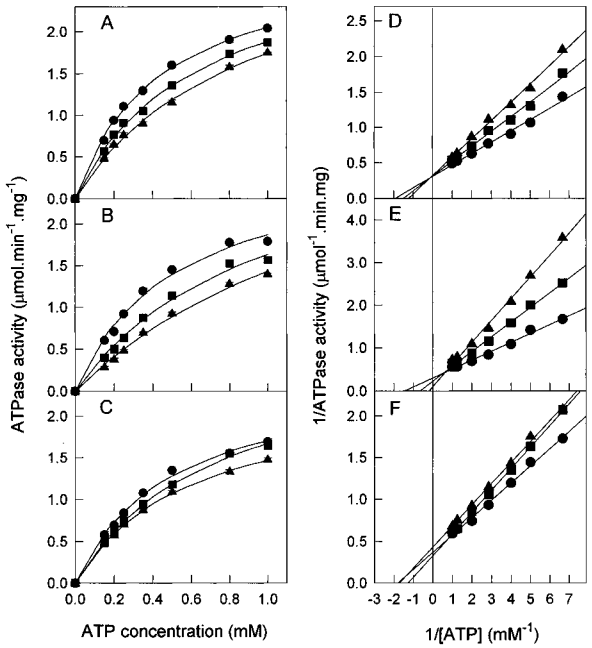

FIGURE 3: Kinetics of inhibition of Pgp-mediated ATP hydrolysis by TNP-nucleotide derivatives. Left panels show Michaelis−Menten plots for inhibition of ATP hydrolysis by purified Pgp in the presence of (A) TNP-ATP (none, ●; 50 μM, ■; 100 μM, ▲, (B) TNP-ADP (none, ●; 25 μM, ■; 50 μM, ▲), and (C) TNP-AMP (none, ●; 100 μM, ■; 200 μM, ▲). Data up to 1.0 mM ATP were fitted to the Michaelis−Menten equation using nonlinear regression analysis; the solid lines indicate the calculated best-fit curves. The corresponding Lineweaver−Burk plots, D (TNP-ATP), E (TNP-ADP), and F (TNP-AMP) are shown in the right panels.

concentration of TNP-ATP (compare Figure 3A and B). TNP-ADP displayed mixed inhibition kinetics (Figure 3E); the inhibition curves were fitted to the Michaelis−Menten equation to obtain values for the apparent K_M for ATP hydrolysis (K_M'). K_M' for ATP increased from 0.53 ± 0.07 mM in the absence of TNP-ADP to 1.0 and 1.65 mM in the presence of 25 and 50 μM TNP-ADP, respectively, while V_{max} also increased from 2.86 to 3.26 and 3.80 μmol min^{-1} (mg of protein)$^{-1}$ at these TNP-ADP concentrations. TNP-AMP, which was a poor inhibitor of ATPase activity compared to TNP-ATP and TNP-ADP, also displayed mixed inhibition kinetics (Figure 3F).

Binding of TNP-Nucleotides to Pgp. TNP-nucleotides alone are weakly fluorescent in aqueous solution, with a λ_{max} of emission of 550 nm in the presence of phospholipids. The quantum yield of these derivatives is greatly enhanced when they are transferred to a hydrophobic environment, such as the nucleotide binding pocket within a protein active site. When TNP-ATP and TNP-ADP interacted with purified Pgp there was a large (4−5-fold) increase in their fluorescence intensity, and the spectrum was blue-shifted by 15 nm (Figure 4A). Similar changes were observed when TNP-ATP was added to either native or MIANS-labeled Pgp (Figure 4B). The decrease in emission λ_{max} to 535 nm for both TNP-ATP and TNP-ADP indicates that the nucleotides are located in a relatively nonpolar environment.

The increase in fluorescence on binding of TNP-ATP and TNP-ADP to Pgp was concentration-dependent and saturable (Figure 5A). The fluorescence enhancement data were fitted to an equation describing interaction of the nucleotides with a single class of binding sites. Both derivatives bound with

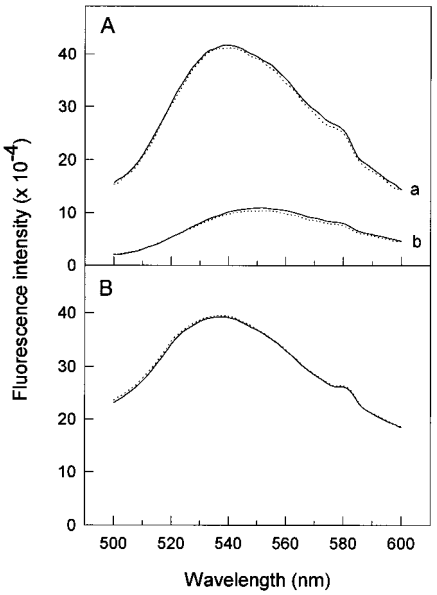

FIGURE 4: Fluorescence emission spectra of TNP-nucleotides in the presence and absence of Pgp. Experiments were carried out at 22 °C, with excitation at 408 nm. (A) TNP-ATP (solid lines) and TNP-ADP (dotted lines) in the presence of 50 μg/mL purified Pgp (a) or in buffer alone (b). (B) Comparison of fluorescence emission spectrum of TNP-ATP in the presence of either native Pgp (solid line), or MIANS-labeled Pgp (dotted line). A control titration was performed in the absence of Pgp, and the fluorescence intensities were subtracted from those recorded in the presence of Pgp. All spectra were recorded in the presence of 0.5 mg/mL phospholipids; emission maxima were not significantly different in their absence.

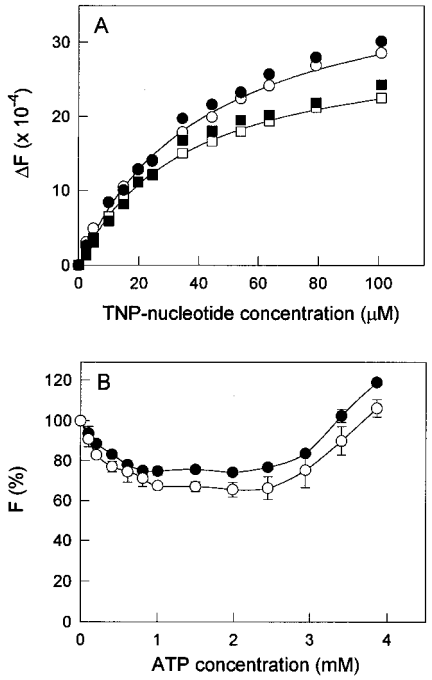

FIGURE 5: Interaction of TNP-nucleotides with Pgp. (A) Binding of TNP-nucleotides to purified Pgp as monitored by enhancement of intrinsic fluorescence. Increasing concentrations of TNP-ATP (●, ○) or TNP-ADP (■, □) were titrated with 50 μg/mL purified Pgp, either native (○, □), or MIANS-labeled (●, ■) in the presence of 0.5 mg/mL phospholipids. (B) Displacement of bound TNP-ATP from Pgp by ATP. Following binding of 30 μM TNP-ATP to purified Pgp, either native (○) or MIANS-labeled (●), the mixture was titrated with increasing concentrations of ATP. Experiments were carried out at 22 °C, with fluorescence emission recorded at 535 nm after excitation at 408 nm. As a control, 30 μM TNP-ATP alone was titrated with increasing concentrations of ATP, and the fluorescence intensity was used to correct the Pgp titration values.

high affinity; K_d values were 43.0 ± 2.8 μM for TNP-ATP binding and 36.2 ± 1.4 μM for TNP-ADP binding. TNP-ATP bound to Pgp with ~10-fold higher affinity than the unmodified nucleotide, for which the K_d was estimated to be 0.46 mM by a fluorescence quenching technique (Liu & Sharom, 1996). MIANS-labeled Pgp displayed fluorescence enhancement curves almost identical to those observed for native Pgp (Figure 5A), which demonstrates that covalent modification of the cysteine residues does not affect binding of the TNP-nucleotide.

When ATP was added to compete off the bound TNP-ATP, the fluorescence was partially reduced, indicating displacement of the fluorescent nucleotide by ATP (Figure 5B). Not all of the TNP-ATP was chased by ATP; this effect may arise from either the existence of some non-specific binding, or the much higher affinity of the fluorescent analog for binding to the NBD. Incomplete displacement of bound TNP-ATP by unlabeled ATP has also been noted for the *E. coli* ArsA protein, another member of the ABC superfamily which extrudes arsenicals (Karkaria & Rosen, 1991). At higher ATP concentrations (>3 mM), fluorescence values increased once more. This type of effect has not been reported for other nucleotide binding proteins and its origin remains obscure. Since high concentrations of ATP are known to be inhibitory for the ATPase activity of purified Pgp (Sharom et al., 1995b), this fluorescence increase may represent the induction of a different "inhibited" conformation of the NBD, which interacts somewhat differently with nucleotides and thus gives rise to increased fluorescence enhancement of the remaining bound TNP-ATP.

Interaction between the MIANS Probe and Bound TNP-Nucleotides. The fluorescence emission spectrum of MIANS bound to Pgp has a high degree of overlap with the excitation spectrum of TNP-ATP and TNP-ADP (λ_{ex}, λ_{em} for MIANS at 322 and 420 nm; λ_{ex}, λ_{em} for TNP-ATP at 408 and 535 nm). There was, therefore, the expectation that fluorescence resonance energy transfer from MIANS (the donor) and TNP (the acceptor) would take place if they were located a suitable distance apart (<40 nm) (Lakowicz, 1983). When MIANS-Pgp was excited at 322 nm in the presence of a concentration of TNP-ATP sufficient to occupy the NBD, fluorescence emission was observed at 535 nm, indicating that energy transfer between the MIANS and TNP moieties had taken place (Figure 6A). The fluorescence emission of the MIANS probe at 420 nm was simultaneously highly quenched. These results provide evidence that the bound TNP-ATP is located relatively close to the MIANS-labeled cysteine residue within the catalytic site of the NBD. Quenching of the MIANS probe by TNP-nucleotides due to resonance energy transfer was concentration-dependent (Figure 6B). Fitting of the data shown in the quench curves to an equation describing binding to a single class of sites gave estimated K_d values for binding of TNP-ATP and TNP-ADP of 40.0 ± 1.9 and 33.3 ± 1.3 μM, respectively. These values are in good agreement with those obtained directly from fluorescence enhancement experiments (Figure 5A).

DISCUSSION

One common feature of active transporters in the ABC superfamily is the coupling of translocation of the transported

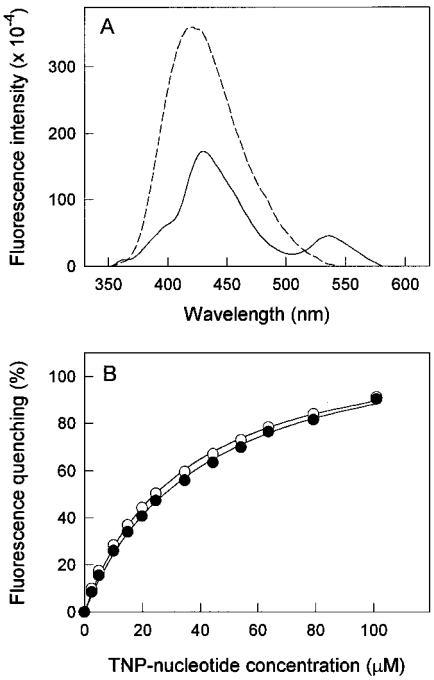

FIGURE 6: Quenching of fluorescence emission by MIANS-Pgp as a result of resonance energy transfer to TNP-nucleotides. (A) Fluorescence emission spectrum of MIANS-labeled Pgp (50 μg/mL in 2 mM CHAPS buffer with 0.5 mg/mL phospholipids) following excitation at 322 nm, in either the absence (dashed line) or presence (solid line) of 30 μM TNP-ATP. (B) Titration of MIANS-labeled Pgp at 22 °C with increasing concentrations of TNP-ATP (●) or TNP-ADP (○). Fluorescence emission of the MIANS group was recorded at 420 nm following excitation at 322 nm.

species to hydrolysis of ATP at two NBDs, whose sequences are highly conserved. Our current understanding of how energy coupling takes place is very limited. Senior and co-workers have shown that, although both NBDs of Pgp are catalytically active (Urbatsch et al., 1995b), nucleotide is trapped by vanadate at only one site during catalysis (Urbatsch et al., 1995a). This led to the suggestion of an "alternating sites" type of mechanism for the two ATPase catalytic domains on Pgp (Senior et al., 1995), in which only one of the two NBDs functions catalytically at a single point in time, in an alternating fashion. Although the role of a few amino acid residues has been explored by site-directed mutagenesis (Gly 431/1073 and Lys 432/1074 in the mouse, and Cys 431/1074 in the human) (Azzaria et al., 1989; Loo & Clarke, 1995b), there is currently no three-dimensional structure available for the NBD. The aim of the present study was to use fluorescence techniques to probe the molecular architecture of the catalytic and nucleotide binding regions within the NBDs of Pgp.

We took advantage of the fact that a conserved Cys residue within each NBD of Pgp can be specifically labeled with the fluor MIANS (Liu & Sharom, 1996). Quenching studies can then be used to report back on the local environment of the fluor. The Stern−Volmer plots for collisional quenching of MIANS-Pgp by acrylamide, I^-, and Cs^+ were all linear. The absence of multiple components indicates the existence of a single class of quenched fluors, which suggests that the two MIANS groups, bound to Cys 428 and Cys 1071 within NBD1 and NBD2, respectively, appear to be located in environments that are virtually identical. The K_{sv} values obtained for acrylamide quenching of MIANS-Pgp (1.42 M^{-1}) vs MIANS-DTE (6.29 M^{-1}) suggest that the MIANS probe is relatively deeply buried within the protein structure following covalent attachment to the cysteine residue in the NBD. This is in keeping with the fact that the emission maximum of MIANS bound to Pgp indicates a relatively hydrophobic environment (Liu & Sharom, 1996). It seems likely that a hydrophobic pocket exists to accommodate the adenine ring of the bound nucleotide. By comparison, the K_{sv} values for acrylamide quenching of MIANS bound to the active site of bovine ferrochelatase (Dailey, 1985), the myosin ATPase (Hiratsuka, 1992), and a location within transmembrane helix X of lactose permease (Wu et al., 1994), are 3.00, 1.1, and 2.88 M^{-1}, respectively.

Further experiments showed that positively and negatively charged quenchers had very different effects on the MIANS probe within the NBD. Highly effective quenching by I^-, in contrast to very poor quenching by Cs^+, implied that the region where the MIANS is located within the NBD is most likely positively charged. This is not unexpected, since positively charged amino acid side chains would be required to bind a highly negatively charged nucleotide efficiently. In this respect, a highly conserved lysine residue is located in each of the Walker A motifs of Pgp and as many as 66 other ABC transporters (Dayan et al., 1996). These lysine residues, which are essential for ATPase activity (Azzaria et al., 1989), are located two residues downstream of the labeled cysteines. It seems likely that these lysine residues make a major contribution to the positively charged character of the ATP binding site.

Occupation of the NBD with ATP resulted in a reduction in the quenching of Pgp-bound MIANS by acrylamide. It appears, therefore, that the conformational change induced by ATP binding produces a significant decrease in the accessibility of the MIANS-labeled cysteine residues to the aqueous environment. The observed reduction in K_{sv} of ~10% is small in comparison with changes observed on binding of ATP to other ATPases; for example, myosin ATPase labeled with MIANS on Cys 697 displayed a 3-fold increase in K_{sv} following ATP binding (Hiratsuka, 1992). Our findings suggest either that the conformational change induced by ATP binding to the NBD of Pgp is relatively minor or that the change in conformation has only a small effect on the solvent accessibility of the probe. ATP binding to Pgp causes a large, concentration-dependent quenching of the MIANS fluorescence (Liu & Sharom, 1996), likely by a direct effect on probe quantum yield, rather than a conformational change.

When the NBD is occupied by ATP, I^- becomes a much less effective quencher, which is in keeping with the idea that the bound nucleotide partially shields the positive charge in the active site region, decreasing the attraction of I^- to this region. ATP may also sterically block the quencher from gaining access to the MIANS group. Quenching by Cs^+ is increased when the NBD is occupied with ATP. This increase in quenching efficiency likely arises from the sum of two effects; partial screening of the lysine residue by the bound nucleotide would allow Cs^+ to approach this region of the active site more readily, thus increasing quenching, while steric hindrance would tend to decrease quenching.

Recombinant versions of both the N-terminal and C-terminal NBD of Pgp have been overexpressed in *E. coli* and purified, either as a fusion protein with glutathione *S*-transferase (Baubichon-Cortay et al., 1994), maltose bind-

ing protein (Sharma & Rose, 1995) or as a 187-amino acid peptide (Dayan et al., 1996). Isolated NBD1 or the glutathione *S*-transferase fusion protein of NBD2 were able to interact with fluorescent nucleotide derivatives, such as TNP-ATP and 2′(3′)-*N*-methylanthraniloyl-ATP. However, in all three cases, the ATPase activity of the expressed proteins was extremely low, 1−25 nmol min^{-1} (mg of protein)$^{-1}$, which is 100−2500-fold lower than the activity of the highly purified Pgp used in the present investigation (Sharom et al., 1995b; Liu & Sharom, 1996). In these previous studies, it was, therefore, not possible to examine whether these nucleotides were substrates for hydrolysis by the recombinant NBD or how they affected Pgp ATPase activity.

The present study showed that TNP-ATP is indeed a substrate for Pgp ATPase, although the bulky TNP group appeared to interfere with hydrolysis, resulting in a V_{max} about 20-fold lower than that obtained using unmodified ATP. Other enzymes that utilize ATP are also able to use TNP-ATP as an alternate substrate; in the case of *E. coli* F_0F_1-ATPase, the rate of hydrolysis was 100-fold lower (Weber & Senior, 1996), whereas for the epidermal growth factor tyrosine kinase, the rate of autophosphorylation was reduced 200-fold (Cheng & Koland, 1996). The V_{max} for TNP-ATP hydrolysis by Pgp relative to ATP is high compared with these examples, and likely reflects the fact that the catalytic sites of Pgp appear somewhat nonspecific, and can tolerate modifications of the nucleotide quite well (Urbatsch et al., 1994).

TNP-ATP and TNP-ADP were both good inhibitors of Pgp ATPase activity. TNP-ATP acted as a classical competitive inhibitor, with a K_i of 111 μM. TNP-ADP was a substantially better inhibitor of ATPase activity than TNP-ATP at the same concentration and behaved as a mixed inhibitor, changing both the K_M and V_{max} for ATP hydrolysis. We previously noted that ADP was a classical competitive inhibitor of Pgp ATPase, with a K_i of 0.2 mM, lower than the K_M for ATP itself (Sharom et al., 1995b). Similar observations were also reported by Urbatsch et al. (1994). It appears that the additional presence of the TNP group confers mixed inhibition kinetics. It is possible that the observed changes in kinetics for TNP-ADP arise from interactions between the two NBDs; binding of TNP-ADP at one site may change the kinetic behavior of the second site. However, this seems unlikely, since such kinetic changes are not seen for unmodified ADP, which is a classical competitive inhibitor of Pgp ATPase activity (Sharom et al., 1995b). Since attachment of the TNP group does not alter the kinetic behavior of ATP, the origins of the complex kinetics noted for TNP-ADP are unclear. TNP-AMP was a poor inhibitor of Pgp ATPase activity; this is expected based on the fact that unmodified AMP is also a poor inhibitor [our observations and Urbatsch et al. (1994)]. In addition, ATP blocks MIANS labeling of Cys 428/1071 very effectively, whereas AMP is unable to do so (Liu & Sharom, 1996), suggesting that it does not occupy the NBD.

TNP-ATP and TNP-ADP bound to Pgp with concomitant enhancement of their intrinsic fluorescence, confirming that the binding site for nucleotides within the NBD has nonpolar character. Binding was of high affinity for both TNP-ATP and TNP-ADP (43 and 36 μM, respectively), which is approximately 10-fold higher than the affinity for the unmodified nucleotides. Measurement of binding affinities by an independent experiment, involving quenching of MIANS fluorescence by bound TNP-nucleotide, gave almost identical values of 40 and 33 μM respectively. In addition, the K_M for hydrolysis of TNP-ATP by Pgp was comparable (81 μM). High-affinity binding has also been reported for interaction of TNP-ATP with the ATP binding sites of other proteins, including the ArsA protein (Karkaria & Rosen, 1991), both NBD1 and NBD2 of the cystic fibrosis transmembrane conductance regulator, CFTR (Randak et al., 1995; Ko et al., 1993), and the epidermal growth factor receptor (Cheng & Koland, 1996).

The two NBDs appear to be able to operate independently of each other, since "half-molecules" of Pgp containing either the N-terminal or C-terminal NBD showed normal levels of ATPase activity (Loo & Clarke, 1994). Both the collisional quenching data, and the TNP-nucleotide binding data presented here gave no indication of two different classes of sites, which implies that NBD1 and NBD2 behave virtually identically. However, it is not known whether both NBDs are able to bind nucleotides simultaneously in full-length Pgp. Unfortunately, it was not possible to measure the stoichiometry of TNP-ATP binding in this study, since the K_d for binding was 40−43 μM, whereas the maximum Pgp concentration that could be achieved was 3−6 μM, which is not sufficient for saturation of the added TNP-ATP.

The low levels of ATPase activity observed for the separately expressed NBD of Pgp might indicate that these domains are not folded properly. However, this seems unlikely, since both domains can still bind fluorescent nucleotide derivatives with high affinity (Baubichon-Cortay et al., 1994; Dayan et al., 1996). A more plausible explanation is that interactions of the two NBDs with either membrane-inserted regions of Pgp, or the membrane itself, may be necessary for catalytic activity. In this respect, the ATPase function of Pgp is known to be highly dependent on membrane phospholipids (Doige et al., 1993; Urbatsch & Senior, 1994; Sharom et al., 1995b), and we have shown that phospholipids can modulate the kinetic parameters of catalysis (Sharom, 1997).

Our findings showed that TNP-nucleotides can bind to MIANS-labeled Pgp with unaltered affinity, despite the presence of the bulky MIANS probe. The two fluors are located relatively close to each other, since fluorescence resonance energy transfer was readily observable and resulted in almost complete quenching of the MIANS group. The labeled Cys residues, although not strictly necessary for catalytic activity of Pgp (Loo & Clarke, 1995a) are, therefore, very near to the site where the nucleotide binds within the NBD. Fluorescence energy transfer experiments are now in progress in our laboratory to determine the distance(s) between bound TNP-nucleotides, the MIANS group attached to Cys 428/1071, and various fluorescent drugs. The results of these new fluorescence approaches will provide important information on the spatial organization of the NBDs relative to the site(s) on Pgp where transport substrates bind.

REFERENCES

Azzaria, M., Schurr, E., & Gros, P. (1989) *Mol. Cell. Biol. 9*, 5289−5297.

Baubichon-Cortay, H., Baggetto, L. G., Dayan, G., & Di Pietro, A. (1994) *J. Biol. Chem. 269*, 22983−22989.

Bradford, M. M. (1976) *Anal. Biochem. 72*, 248−254.

Cheng, K., & Koland, J. G. (1996) *J. Biol. Chem. 271*, 311−318.

Dailey, H. A. (1985) *Biochemistry 24*, 1287−1291.

Dayan, G., Baubichon-Cortay, H., Jault, J.-M., Cortay, J.-C., Deléage, G., & Di Pietro, A. (1996) *J. Biol. Chem. 271*, 11652−11658.
Doige, C. A., & Sharom, F. J. (1991) *Protein Express. Purific. 2*, 256−265.
Doige, C. A., & Ames, G. F. (1993) *Annu. Rev. Microbiol. 47*, 291−319.
Doige, C. A., Yu, X., & Sharom, F. J. (1992) *Biochim. Biophys. Acta 1109*, 149−160.
Doige, C. A., Yu, X., & Sharom, F. J. (1993) *Biochim. Biophys. Acta 1146*, 65−72.
Eytan, G. D., Borgnia, M. J., Regev, R., & Assaraf, Y. G. (1994) *J. Biol. Chem. 269*, 26058−26065.
Gottesman, M. M., & Pastan, I. (1993) *Annu. Rev. Biochem. 62*, 385−427.
Higgins, C. F. (1992) *Annu. Rev. Cell Biol. 8*, 265−269.
Hiratsuka, T. (1992) *J. Biol. Chem. 267*, 14941−14948.
Karkaria, C. E., & Rosen, B. P. (1991) *Arch. Biochem. Biophys. 288*, 107−111.
Ko, Y. H., Thomas, P. J., Delannoy, M. R., & Pedersen, P. L. (1993) *J. Biol. Chem. 268*, 24330−24338.
Lakowicz, J. R. (1983) *Principles of Fluorescence Spectroscopy*, Plenum Press, New York.
Lehnert, M. (1996) *Eur. J. Cancer 32A*, 912−920.
Leveille-Webster, C. R., & Arias, I. M. (1995) *J. Membr. Biol. 143*, 89−102.
Ling, V., & Thompson, L. H. (1974) *J. Cell. Physiol. 83*, 103−116.
Liu, R., & Sharom, F. J. (1996) *Biochemistry 35*, 11865−11873.
Loo, T. W., & Clarke, D. M. (1994) *J. Biol. Chem. 269*, 7750−7755.
Loo, T. W., & Clarke, D. M. (1995a) *J. Biol. Chem. 270*, 843−848.
Loo, T. W., & Clarke, D. M. (1995b) *J. Biol. Chem. 270*, 22957−22961.
MacDonald, R. C., MacDonald, R. I., Menco, B. P. M., Takeshita, K., Subbarao, N. K., & Hu, L.-R. (1991) *Biochim. Biophys. Acta 1061*, 297−303.
Peterson, G. L. (1983) *Methods Enzymol. 91*, 95−119.
Randak, C., Roscher, A. A., Hadorn, H.-B., Assfalg-Machleidt, I., Auerswald, E. A., & Machleidt, W. (1995) *FEBS Lett. 363*, 189−194.
Schinkel, A. H., Wagenaar, E., van Deemter, L., Mol, C. A. A. M., & Borst, P. (1995) *J. Clin. Invest. 96*, 1698−1705.
Schinkel, A. H., Wagenaar, E., Mol, C. A. A. M., & van Deemter, L. (1996) *J. Clin. Invest. 97*, 2517−2524.
Senior, A. E., Al-Shawi, M. K., & Urbatsch, I. L. (1995) *FEBS Lett. 377*, 285−289.
Shapiro, A. B., & Ling, V. (1994) *J. Biol. Chem. 269*, 3745−3754.
Shapiro, A. B., & Ling, V. (1995) *J. Biol. Chem. 270*, 16167−16175.
Sharma, S., & Rose, D. R. (1995) *J. Biol. Chem. 270*, 14085−14093.
Sharom, F. J. (1995) *J. Bioenerg. Biomembr. 27*, 15−22.
Sharom, F. J. (1997) *Biochem. Soc. Trans.*, in press.
Sharom, F. J., Yu, X., & Doige, C. A. (1993) *J. Biol. Chem. 268*, 24197−24202.
Sharom, F. J., DiDiodato, G., Yu, X., & Ashbourne, K. J. D. (1995a) *J. Biol. Chem. 270*, 10334−10341.
Sharom, F. J., Yu, X., Chu, J. W. K., & Doige, C. A. (1995b) *Biochem. J. 308*, 381−390.
Sharom, F. J., Yu, X., DiDiodato, G., & Chu, J. W. K. (1996) *Biochem. J. 320*, 421−428.
Urbatsch, I. L., & Senior, A. E. (1994) *Arch. Biochem. Biophys. 316*, 135−140.
Urbatsch, I. L., Al-Shawi, M. K., & Senior, A. E. (1994) *Biochemistry 33*, 7069−7076.
Urbatsch, I. L., Sankaran, B., Weber, J., & Senior, A. E. (1995a) *J. Biol. Chem. 270*, 19383−19390.
Urbatsch, I. L., Sankaran, B., Bhagat, S., & Senior, A. E. (1995b) *J. Biol. Chem. 270*, 26956−26961.
Walker, J. E., Saraste, M., Runswick, M. J., & Gay, N. J. (1982) *EMBO J. 1*, 945−951.
Weber, J., & Senior, A. E. (1996) *J. Biol. Chem. 271*, 3474−3477.
Wu, J., Frillingos, S., Voss, J., & Kaback, H. R. (1994) *Protein Sci. 3*, 2294−2301.

BI9627119